PERGAMON

Applied Radiation and Isotopes 51 (1999) 543–549

Applied Radiation and Isotopes

www.elsevier.com/locate/apradiso

Modeling rhenium-186 and rhenium-188 distribution in a neutron-activated rhenium wire and effect of the distribution on beta dosimetry in a water phantom

William K. Roberts, Urs O. Häfeli*

The Cleveland Clinic Foundation, Radiation Oncology Department T28, 9500 Euclid Avenue, Cleveland, OH 44195, USA

Received 24 February 1999; accepted 29 March 1999

Abstract

Radioactive β-emitting rhenium wire brachytherapy sources produced by neutron activation in an isotropic thermal neutron field have a non-uniform radial radioisotope distribution. We modeled this distribution and confirmed the model by experimental measurements on wires of 0.1–1.0 mm diameter. When the corrected radial distributions of ^{186}Re and ^{188}Re were used, the calculated dose distribution around a 0.5-mm wire agreed with the distribution measured with Gafchromic film in a solid water phantom to within 5.0% over the therapeutic range (radius of 0.4–2.8 mm).

Keywords: Wire brachytherapy source; β emitter; ^{186}Re; ^{188}Re; Neutron activation; γ-Ray assay

1. Introduction

In up to 40% of the 400,000 patients treated with balloon coronary angioplasty in the US every year, the blood vessels restenose (Holmes et al., 1984). Ionizing radiation applied from within the vessel (endovascular brachytherapy) is able to reduce the incidence of restenosis after balloon angioplasty. In two clinical trials, investigators were able to decrease the incidence of restenosis after 1 year from 54% (Teirstein et al., 1997) to 15% and 17%, respectively (King et al., 1998; Teirstein et al., 1997).

Different radioactive sources can be used for endovascular brachytherapy. Teirstein et al. used a ^{192}Ir γ-source, whereas King et al. treated with a ^{90}Sr/^{90}Y β-source. We are interested in β-sources which are easier to shield and have a well-defined range that limits toxicity to tissue surrounding the vessel. We recently investigated the feasibility of a rhenium wire source for preventing restenosis. Dosimetric measurements on a 0.5 mm-diameter metallic rhenium source showed that it could deliver the necessary doses of 15–18 Gy to vessels with diameters up to 6 mm (Häfeli et al., 1999). Further reasons for chosing rhenium was its good radiochemical stability, which makes the direct use of very small source wires or coils down to 0.1 mm diameter possible, and because it is highly visible under fluoroscopy. The radioactive rhenium source is produced in a reactor by thermal neutron capture in naturally occurring rhenium isotopes. The two radioactive rhenium isotopes produced (^{186}Re and ^{188}Re) are mainly β-emitters, but also emit some γ-rays (see Table 1).

* Corresponding author. Tel.: +1-216-444-2174; fax: +1-216-445-4480.

E-mail address: hafeliu@ccf.org (Urs O. Häfeli)

0969-8043/99/$ - see front matter
PII: S0969-8043(99)00080-9

Table 1
Properties of radioactive rhenium[a]

	Rhenium-186	Rhenium-188
Natural abundance of the precursor[b]	37.4% (^{185}Re)	62.6% (^{187}Re)
Cross-section for neutrons σ_{cap}	$112 \pm 2 \times 10^{-24}$ cm^2 (^{185}Re)	$76.4 \pm 1.0 \times 10^{-24}$ cm^2 + 2.8[c] $\pm 0.1 \times 10^{-24}$ cm^2 (^{187}Re)
Scattering cross-section for neutrons σ_{scat}	$10.6 \pm 0.6 \times 10^{-24}$ cm^2 (^{185}Re)	$11.8 \pm 0.4 \times 10^{-24}$ cm^2 (^{187}Re)
Average/maximum β-energy	346.7/1069.5 keV	764.3/2120.4 keV
Maximum β-range in tissue	5.0 mm	11.0 mm
Major γ-ray energy (abundance)	137.2 keV (9.42 ± 0.06%)	155.0 keV (15.1 ± 0.004%)
Half-life	89.24 ± 0.03 h (3.7 d)	17.005 ± 0.004 h (0.7 d)

[a] Data from Nudat (1998).
[b] Weast (1988).
[c] meta-stable product ^{188m}Re.

To calculate the dose fall-off around beta wire sources of different diameters, to account for the effects of different materials surrounding the source (such as the catheter material and contrast media), and to gauge the effects of differences in geometry (such as catheter wall thickness), we developed BETA, a Monte Carlo-based computer program simulating electron transport. This program, given a precise measure of the radioactive source distribution, calculates the dose delivered by an annular β-source to surrounding material. To measure the source distribution, we assay the radioactive wires for ^{186}Re and ^{188}Re activity using a NIST-calibrated high-resolution germanium γ-ray detection system. This simple assay assumes that the γ-rays reach the detector from their emission point within the wire with neither Compton nor photoelectric interactions with the rhenium before reaching the detector. We assumed initially that the activity measured in the simple assay was uniformly distributed throughout the wire. However, we found that the calculated doses were generally much lower than the experimentally determined ones.

Investigation of this problem led us to the conclusion that BETA worked properly, but that 2 factors are responsible for the deviation. First, wire material with large thermal neutron interaction cross-section, when activated by thermal neutrons, will produce a radially varying distribution of activity. Second, γ-rays originating from within the wire will interact with the wire material, undergoing Compton and photoelectric interactions, so that the simple assay underestimates the true activity in the wire. In this paper, we report formulae that correct for these effects so that the radial distribution of activity in a wire brachytherapy source can be accurately calculated from the results of a simple assay. We also test our formulae by comparing predicted dose distributions with observed dose distributions in a solid water phantom for wires of different diameters.

2. The model

In this section, we first develop a model of $A_i(r,r_0)$, the radial distribution of the specific activity of isotope i within a wire exposed to a thermal neutron flux, where r_0 is the wire radius and r is the distance from the center of the wire to the location of thermal neutron capture. The model predicts that the activity will decrease monotonically from the wire surface to the wire center. Next, we model the probability that a photon emitted from within the wire in a direction to be detected escapes both Compton interactions which reduce the photon energy and photoelectric interactions which eliminate the γ-rays in the intervening wire material. The models are then combined to generate an escape factor $P_{esc}(r_0)$. We then show how the radial distribution can be calculated from simple measurements made with a NIST-calibrated high-resolution germanium γ-ray detection system. The decay of the rhenium isotopes is accompanied by γ-rays which can be detected in the Ge-detector with an efficiency $\varepsilon(E)$ where E is the γ-ray energy. Each γ-ray has a probability $f_i(E)$ of accompanying a rhenium decay [$f_i(E)$ is usually < 1]. The apparent specific activity, $AA_i(r_0)$, is calculated by dividing this adjusted measured activity by the wire mass and by the time the wire was in the reactor at a known flux. Then $A_i(r,r_0)$ can be calculated from this value as described below. Once $AA_i(r_0)$ has been measured, the true specific activity, $A_i(r,r_0)$, can be calculated as outlined below.

Three basic assumptions were used in the modeling. First, the thermal flux is uniform, completely isotropic, linearly dependent on the reactor power level, and unaffected by the insertion of sample material within a prescribed volume of the reactor. Second, the wire's length is great compared to its radius, making end effects negligible. And last, the irradiation time T_{irr} is much shorter than the half-life of the radioisotopes of interest.

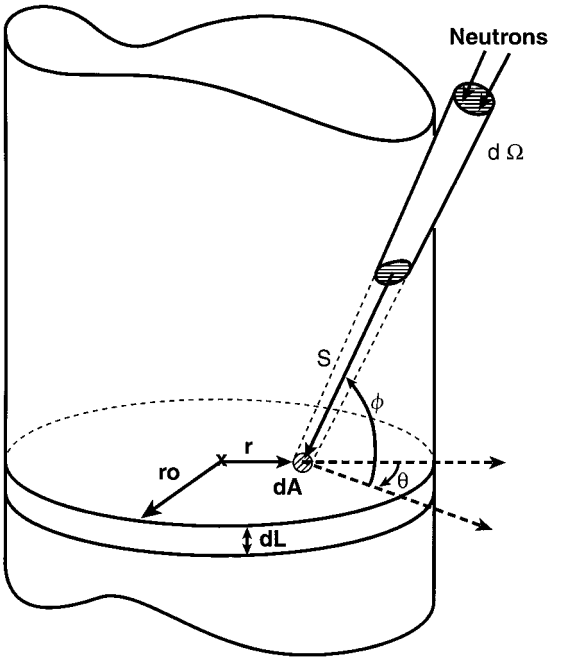

Fig. 1. Schematic drawing of the neutron activation process. The thermal neutrons arrive at a small volume $dA \times dL$ located at a radius r on a cylindrical slice of thickness dL from a solid angle element $d\Omega$ after traveling a distance S within the wire. Angles θ and ϕ define the arrival direction of neutrons at the elemental volume.

2.1. Calculation of the radial specific activity

We will first calculate ${}^0A_i$, the specific activity produced in a pillbox-shaped, vanishingly small volume ($dA \times dL$) of wire material if it were placed in the reactor at the wire irradiation position. The specific activity in this volume ${}^0A_i$ (Bq/mg/s of neutron activation) is a function of the isotope decay constant λ_i (s^{-1}), the thermal neutron flux per steridian F, the weight fraction w_i of the rhenium isotope with which the neutrons interact, its molecular weight MW_i, the isotope-specific capture cross-section σ_i (measured in barns where 1 barn = 10^{-24} cm^2), and Avogadro's number N_a (6.022×10^{23}). ${}^0A_i$ is calculated in Eq. (1). Note that ${}^0A_i$ is a constant for the isotope i.

$$ {}^0A_i = \frac{\lambda_i \times F \times w_i \times \sigma_i \times N_a}{MW_i} \int_0^{4\pi} d\Omega = \frac{\lambda_i \times F \times w_i \times \sigma_i \times N_a}{MW_i} \times 4 \times \pi. \quad (1) $$

In a wire, neutrons arrive at a small volume located at radius r on a cylindrical slice of thickness dL from a solid angle element $d\Omega$ after traveling a distance S within the wire as shown in Fig. 1. The path length S can be calculated as a function of θ, ϕ, r, and r_0:

$$ S = \frac{-r \times \cos(\theta) + \sqrt{(r \times \cos(\theta))^2 - r^2 + r_0^2}}{\cos(\phi)}. \quad (2) $$

The probability that a thermal neutron will escape capture while traversing the path S is

$$ P_s = e^{-\sigma_{tot} \times n \times S} \quad (3) $$

where σ_{tot} is the total interaction cross-section in natural rhenium and n is the number of rhenium nuclei per volume (in cm^3). The escape probability is thus proportional to the density $\rho = n \times MW/(N_a \times V)$. The specific activity in a long wire, $A_i(r,r_0)$, can be calculated by including the probability of neutron survival to that point in the wire in the integral of Eq. (1). The solid angle element is $d\Omega = d\phi \times d\theta \times \cos(\phi)$.

$$ A_i(r, r_0) = \frac{\lambda_i \times F \times w_i \times \sigma_i \times N_a}{MW_i} \times 2 \int_0^{\pi} d\theta \times 2 \int_0^{\pi/2} d\phi \times \cos(\phi) \times P_s = \frac{{}^0A_i}{\pi} \int_0^{\pi} d\theta \int_0^{\pi/2} d\phi \times \cos(\phi) \times P_s. \quad (4) $$

The normalized radial distribution $V(r,r_0)$ is defined in Eq. (5).

$$ V(r, r_0) = \frac{A_i(r, r_0)}{{}^0A_i} = \frac{1}{\pi} \times \int_0^{\pi} d\theta \int_0^{\pi/2} d\phi \times \cos(\phi) \times P_s. \quad (5) $$

Normalized radial distributions for 4 wire radii are presented in Fig. 2.

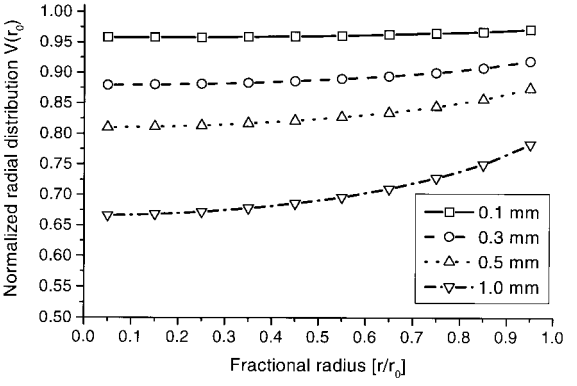

Fig. 2. Normalized radial distributions $V(r,r_0)$ as defined in Eq. (5) were calculated for 4 wire diameters using a neutron total capture cross-section of 95 barns.

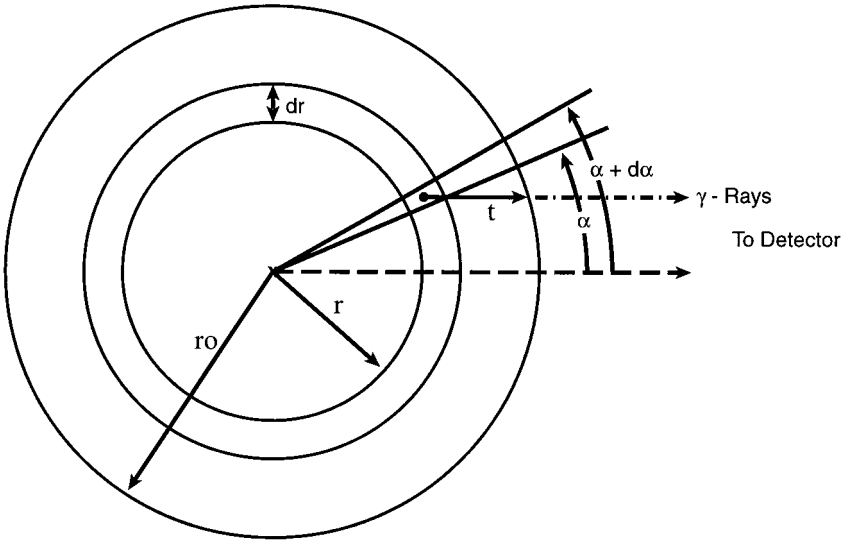

Fig. 3. Geometry employed in modeling the escape of γ-rays from a small volume $dr \times r \times d\alpha \times dL$ located at an angle α from the γ-ray detection system central axis and a distance r from the wire slice center. The γ-rays travel the distance t in the wire material.

2.2. Calculation of the γ-ray escape probability from a rhenium wire

The "apparent specific activity", $AA_i(r_0)$, is calculated using Eq. (6) where $R(E)$ is the γ-ray-specific detection rate (γ-rays detected per second per mg of wire per second of neutron irradiation), $\varepsilon(E)$ is the detection efficiency for that γ-ray in the existing geometry, and $f_i(E)$ is the number of nuclear γ-rays per decay (Photcoef, 1996).

$$AA_i(r_0) = \frac{R(E)}{\varepsilon(E) \times f_i(E)}. \tag{6}$$

γ-rays emanating from any elemental volume in a thin slice of the wire would be detected with very nearly the same efficiency if there were no γ-ray interactions before the rays escaped from the wire. The probability that a γ-ray emitted from this volume element will escape the wire in a direction to be detected (see Fig. 3) is:

$$P_{esc} = e^{-\mu(E)\times t} \tag{7}$$

where $-\mu(E)$ is the sum of the Compton and photoelectric linear absorption cross-sections for rhenium at a photon energy of E. The expected detection rate $R(r_0)$ from this slice is calculated by integration Eq. (8):

$$R(r_0) = \frac{2 \times \varepsilon(E) \times F(E)}{\pi \times r_0^2} \int_0^{r_0} dr \times \int_0^{\pi} r \times d\alpha \times AA_i(r, r_0) \times e^{-\mu(E)\times t} \tag{8}$$

where

$$t = r \times \cos(\alpha) - \sqrt{r_0^2 - (r \times \cos(\alpha))^2} \quad 0 < \alpha \leqslant \pi/2$$

$$t = r \times \cos(\alpha) + \sqrt{r_0^2 - (r \times \cos(\alpha))^2} \quad \pi/2 < \alpha \leqslant \pi$$

$$A_i(r, r_0) = {}^0A_i \times V(r, r_0).$$

An escape probability $P_{esc}(r_0,E)$ is defined as:

$$P_{esc}(r_0, E) = \frac{2}{\pi \times r_0^2} \int_0^{r_0} dr \times r \int_0^{\pi} d\alpha \times V(r, r_0) \times e^{-\mu(E)\times t} \tag{9}$$

and hence the expected apparent specific activity for a wire of radius r_0 is:

$$AA_i(r_0) = {}^0A_i \times P_{esc}(r_0, E). \tag{10}$$

The radial specific activity $A_i(r,r_0)$ can be calculated from $AA_i(r_0)$ and the calculated values of $V(r,r_0)$ using Eq. (11):

$$A_i(r, r_0) = {}^0A_i \times V(r, r_0) = \frac{AA_i(r, r_0) \times V(r, r_0)}{P_{esc}(r_0, E)}. \tag{11}$$

2.3. Calculation of the average specific activity

Another factor of interest is the average specific activity of the wire, ${}^{avg}A_i$. It is specific activity that

Table 2
Calculated and observed* values of different variables for radioactive rhenium wires

Wire diameter (mm)	$^{avg}V(r_0)$	Rhenium-186			Rhenium-188		
		$AA_{186}(r_0)$* (kBq/mg/s)	$P_{esc}(r_0,137)$	$^0A_{186}(r_0)$ (kBq/mg/s)	$AA_{188}(r_0)$* (kBq/mg/s)	$P_{esc}(r_0,155)$	$^0A_{188}(r_0)$ (kBq/mg/s)
0.1	0.960	0.659 ± 0.029	0.816	0.808 ± 0.036	3.13 ± 0.24	0.852	3.87 ± 0.30
0.3	0.890	0.445 ± 0.014	0.565	0.788 ± 0.025	2.57 ± 0.13	0.633	4.06 ± 0.20
0.5	0.829	0.329 ± 0.012	0.408	0.806 ± 0.029	1.97 ± 0.04	0.483	4.08 ± 0.08
1.0	0.705	0.168 ± 0.005	0.213	0.789 ± 0.023	1.08 ± 0.02	0.273	3.96 ± 0.09

would be measured if a wire were dissolved and then deposited as a thin layer and assayed. The layer is assumed to be so thin that negligible Compton or photoelectric interactions occur, i.e. a zero-thickness source. $^{avg}A_i(r_0)$ is calculated in Eq. (12):

$$^{avg}A_i = \int_0^{r_0} \frac{2 \times r \times dr}{r_0^2} \times A_i(r, r_0) = {}^0A_i \times {}^{avg}V(r_0) \quad (12)$$

where

$$^{avg}V(r_0) = \int_0^{r_0} \frac{2 \times r \times dr}{r_0^2} \times V(r, r_0).$$

The values for $P_{esc}(r_0,E)$ [see Eq. (9)] and $^{avg}V(r_0)$ [see Eq. (12)] were evaluated by numerical integration and tabulated in Table 2 for the same 4 wire radii noted in Fig. 2. The total thermal neutron interaction cross-section used in our calculation was 95 barns. In the numerical integration of Eq. (9), the steps in r and α were decreased until the value of $P_{esc}(r_0,E)$ was within 0.01% of 1 when both $V(r,r_0)$ and P_{esc} were set equal to 1. Similar criteria were employed in the evaluation of Eqs. (5) and (12).

3. Experimental methods

3.1. Neutron activation

To verify the model, metallic rhenium wires of diameters of 0.1, 0.3, 0.5, and 1.0 mm were exposed to thermal neutrons at the research reactor of the Ohio State University, Columbus, OH and assayed with a high-purity germanium detector and multi-channel analyzer (EG&G Ortec, Oak Ridge, TN) calibrated for various geometries with a NIST-traceable multiple energy γ-ray source.

Simple assays were performed within 1 h after the end of the irradiation and the results were adjusted to reflect the activity at the moment the wire was removed from the reactor. The thermal neutron fluxes were monitored with cobalt wires and had a value of 2.1×10^{12} neutrons/cm^2/s in the rabbit port at a reactor power of 500 kW. Three separate series of irradiations were performed and the average "apparent specific activity" AA_i (r_0) for each wire diameter determined.

We assayed a portion of a 0.1 mm diameter wire, dissolved it in 10 M HNO_3 at 60°C, buffered to neutral pH, deposited it on a filter paper to create a zero-thickness source, and assayed it again. This was performed on three different wires. The apparent specific activities were determined before and after dissolving the wire. Employing Eq. (12), we calculated the expected filter paper apparent specific activity from the activity measured before the dissolution. Six measurements were made, 3 for ^{186}Re and 3 for ^{188}Re.

3.2. Dosimetric measurement

Gafchromic film (Nuclear Associates, Carle Place, NY) consists of a thin, transparent polyester sheet embedding a chromophore that turns dark blue under the influence of radiation (Chu et al., 1990; McLaughlin et al., 1996). Gafchromic film was calibrated with doses ranging from 0 to 200 Gy using the 6 MV photons from a Varian Clinac 2100-C (Varian Oncology Systems, Palo Alto, CA) linear accelerator. A 4 cm × 4 cm × 0.26 mm piece of Gafchromic film type MD-55 was carefully placed between the 2 layers of a solid water phantom. A 1.7 cm long, 0.5 mm diameter radioactive rhenium wire containing 1040 MBq of ^{188}Re and 488 MBq of ^{186}Re was inserted perpendicularly through a small central drill hole. The rhenium wire of 99.99% purity (Rhenium Alloys, Cleveland, OH) had been neutron-activated 30 h earlier for 20 min at a flux of 1.5×10^{13} n/cm^2/s. Because Gafchromic film has a relatively low sensitivity, we exposed it for 77 minutes (single measurement). The Gafchromic film was scanned at 300 dpi with an X-ray scanner (VXR-12; Vidar Systems Corp., Herndon, VA) to obtain the radiation dose distribution curve. The resulting dose distribution was normalized to an exposure time of 4 min to simulate clinical treatment times.

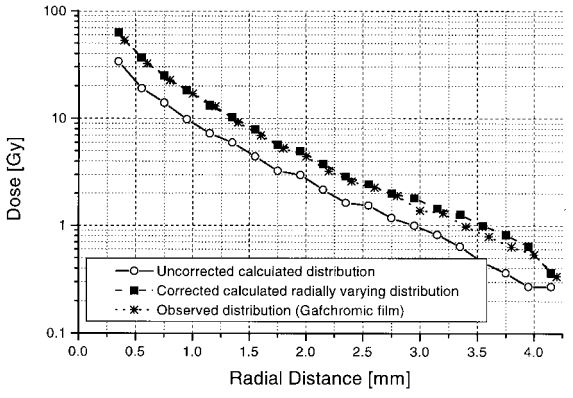

Fig. 4. Dose fall-off from a radioactive wire of 0.5 mm diameter as determined by (a) Gafchromic film measurement, (b) simulation using the apparent activity, and (c) simulation using the actual activity corrected with the source distribution and γ-ray escape factor.

3.3. Monte Carlo-based dose distribution calculation

Our Monte Carlo-based program, BETA, calculates the dose delivered by a radially symmetric annular β-source having a length L and minor and major radii r_1, r_2 located in an infinitely long cylinder of radius R_S ($r_2 \leqslant R_S$). The source region is surrounded by an infinite cylindrical annulus of minor and major radii R_S and R_L and by a region of interest which is all space outside R_L. Each region ($0 \rightarrow R_S$, $R_S \rightarrow R_L$, $R > R_L$) can be modeled as a material of choice, including water, air, muscle, or rhenium. A full description of BETA will be forthcoming. BETA was used to calculate the β-ray dose distributions from the above radioisotope mix of ^{186}Re and ^{188}Re during 4 min of irradiation with the rhenium wire source. Two calculations were performed, one using the average apparent specific activity based on the simple assay, the second using the corrected radial specific activity based on the method reported above.

4. Results and discussion

The average "apparent specific activities" for rhenium wires with diameters of 0.1, 0.3, 0.5, and 1.0 mm, as calculated from the results of 3 irradiations and simple assays per wire diameter, are given in Table 2. As predicted by Eq. (10), $^{0}A_{186}$ and $^{0}A_{188}$, which are equal to the apparent specific activity $AA_i(r_0)$ divided by the γ-ray escape factors $P_{esc}(r_0,E)$ shown in Table 2, are constants independent of wire diameter. Our results thus agree with the model used to obtain $P_{esc}(r_0)$ and $^{avg}V(r_0)$.

The ratio of the apparent specific activity calculated from actual measurements after dissolving 6 wires and depositing them on filter paper to create a zero-thickness source, and the apparent specific activities' predicted values ($\pm$SD) was 1.009 ± 0.047. This is not statistically different from the expected value of 1.000 ($P = 0.69$, 2-tailed t-test).

Fig. 4 plots the dose distribution of the 0.5 mm rhenium wire (a) as measured from Gafchromic film, (b) as calculated by BETA using the apparent specific activity, and (c) as calculated by BETA using the correction methods described in this paper. The corrected calculated dose distribution agrees with the experimentally determined one to within 5.0% over a radial range of 0.4–2.8 mm (the range of radii likely to be used clinically). In contrast, the uncorrected dose distribution calculated from the results of the simple assay is about 50% of the experimentally determined dose. Our measurements and calculations thus show that a simple assay of brachytherapy sources will not automatically lead to correctly calculated dose distributions when Monte Carlo electron distribution type codes are used. A knowledge of the absolute specific activity throughout the source volume is required, and this becomes especially important if the assay is performed with the aid of low energy γ-rays and the source is embedded in a high Z matrix.

The described approach can be used for other β-emitters, however, a more sophisticated approach will be necessary to handle brachytherapy sources that bend sharply, e.g. coils, or when sources are used that have a significant component of low energy γ- and X-rays. For this paper, the γ-ray dose from a ^{186}Re and ^{188}Re source was estimated to be negligible within a radius of 3–4 mm.

5. Conclusion

The equations modeled herein can be used to calculate the true radial distribution of activity produced in a long wire or cylindrical sample after exposure to a uniform thermal neutron flux for which an "apparent specific activity" has been determined. Our program should be of assistance in determining true activity whenever nuclear γ-rays are employed in the assay of long cylindrical samples, providing the radial distribution is known or calculable and uniform along the length of the sample.

Acknowledgements

We would like to thank Joe Talnagi, Jeff Davis and Rick Myser from the Ohio State University reactor, Columbus, OH for activating all the rhenium samples and patiently helping us with all the calibration and

neutron activation details. We are also grateful to Don Evancic for creating the dosimetry phantoms.

References

Chu, R.D.H., Van Dyk, G., Lewis, D.F., O'Hara, K.P.J., Buckland, B.W., et al., 1990. Gafchromic dosimetry media: a new high dose, thin film routine dosimeter and dose mapping tool. Radiat. Phys. Chem 35, 767–773.

Häfeli, U.O., Lee, E.J., Ciezki, J., Pauer, G.J., Weinhous, M.S., 1999. Suitability of beta-emitting rhenium for inhibiting restenosis in coronary arteries. J. Brachytherapy Int 15, 1–11.

Holmes, D.R., Vlietstra, R.E., Smith, H.C., Vetrovec, G.W., Kent, K.M., et al., 1984. Restenosis after PTCA: a report from the PTCA registry of the National Heart, Lung and Blood Institute. Am. J. Cardiol 53, 77C–81C.

King, S.B., Williams, D.O., Chougule, P., Klein, J.L., Waksman, R., et al., 1998. Endovascular beta radiation to reduce restenosis after coronary balloon angioplasty: results of the beta energy restenosis trial (BERT). Circulation 97, 2025–2030.

McLaughlin, W.L., Al-Sheikhly, M., Lewis, D.F., Kovacs, A., Wojnarovits, L., 1996. Radiochromic solid-state polymerization reaction. In: Clough, R.L., Shalaby, S.W. (Eds.), Irradiation of Polymers. American Chemical Society, Washington, DC, pp. 152–166.

NuDAT, 1996. Nuclear Data from NuDat, maintained by the National Nuclear Data Center and IAEA, Brookhaven National Laboratory, [http://www.nndc.bnl.gov/nndc/nudat/] (accessed 27 January, 1999).

Photcoef, 1998. Compton and photo-electric mass absorption coefficients, a compilation of data published by the National Bureau of Standards, the Los Alamos Scientific Laboratory, and by the Kaman Sciences Corporation, [http://www.photcoef.com/212.html] (accessed 27 January, 1999).

Teirstein, P.S., Massullo, V., Jani, S., Popma, J.J., Mintz, G.S., et al., 1997. Catheter-based radiotherapy to inhibit restenosis after coronary stenting. New England Journal of Medicine 336, 1697–1703.

Weast, R.C. (Ed.), 1988. CRC Handbook of Chemistry and Physics, 1st student ed. CRC Press, Boca Raton, FL.